BIBECHANA
A Multidisciplinary Journal of Science, Technology and Mathematics
ISSN 2091-0762 (Print), 2382-5340 (0nline)
Journal homepage: http://nepjol.info/index.php/BIBECHANA
Publisher: Research Council of Science and Technology, Biratnagar, Nepal

Mixing properties of Ni-Al liquid alloys at different temperatures

S. K. Yadav[1*], P. Sharma[2], R. P. Koirala[2], A. Dhungana[2], D. Adhikari[2]
[1]Department of Physics, Suryanarayan Satyanarayan Morbaita Yadav Multiple Campus, Tribhuvan University, Siraha, Nepal.
[2]Department of Physics, Mahendra Morang Adarsh Multiple Campus, Tribhuvan University, Biratnagar, Nepal.
*E-mail: yadavshashit@yahoo.com

Article history: Received 6 September, 2018; Accepted 25 September, 2018
DOI: http://dx.doi.org/10.3126/bibechana.v16i0.21138

Abstract

The validity of simple statistical model or simple theory of mixing has been first established by explaining the experimental values of the thermodynamic and structural properties of Ni-Al melt at 1873 K. Secondly, the linear temperature dependence of ordering energy parameter has been assumed to extend the model for predicting the mixing behaviours of the melt at different temperatures in correlation with R-K polynomials. The surface tension of the system has been explained and predicted with the help of Renovated Butler model. Theoretical investigations correspond that alloy is found to be strongly interacting or hetero-coordinating at its melting temperature. This tendency, however, gradually decreases at higher temperatures. Being more specific, the system shows ideal behaviours with respect to mixing properties at elevated temperatures.

Keywords: Mixing behaviours, Renovated Butler model, hetero-coordinating, surface tension.

1. Introduction

Alloying phenomenon has been evolved as a robust tool in the field of material science and engineering in order to develop new materials with predetermined characteristics. As a result, the alloys have numerous uses in household, industrial, medicinal, military and commercial fields. Similarly, Ni-Al being super alloy has high thermal conductivity, high melting temperature, low density, offers good resistance to oxidation and corrosion and accessible costs. Due to which they have profound utilizations in the modern day technological devices [1, 2]. The details of the uses of the alloy can be found from references 1 and 2. Moreover, the thermal processing routes together with the governing parameters, such as pressure,

temperature and micro-granules determine the microstructure of an alloy. The in-depth understanding of the mixing properties of the initial melts of alloy is thus mandatory in this field. This information cannot be exclusively obtained from the experimental measurements only as being expensive, time consuming, tedious and often face difficulties with regard to the reactivity of the walls of the container at high temperatures [3]. Even to perform experimental measurements, most of the governing parameters are computed by theoretical approximations. With due regards, several theoretical models [1, 3-18] so far have been developed to explain and predict the mixing properties of binary liquid alloys at a temperature or different temperatures. We, therefore, intend to study and explain thermodynamic, structural and transport properties of Ni-Al liquid alloy at 1873 K on the basis of simple theory of mixing (STM) in this work. The surface tension and surface segregation of the alloy have been explained using Renovated Butler model (RBM) [3, 14, 19].

The desirable properties and multi-disciplinary uses of Ni-Al alloy, as stated earlier, have drawn considerable attentions of the several researchers [1, 2, 20-27] working in the field of material science. Ansara et al. (1988) compared the different thermodynamic model to compute the different phases of Ni-Al alloy and concluded that the results obtained from sub-lattice model are more close to experimental predictions. Maret et al. (1990) have determined the Bhatia-Thornton and Faber-Ziman structure factors by neutron diffraction method for $Al_{80}Ni_{20}$ liquid alloy. Their work further corresponds that the chemical short-range order is quite more prominent in $Al_{80}Ni_{20}$ than in $Al_{80}[Mn_x(FeCr)_{1-x}]_{20}$ phase. Pasturel et al. (1992) have shown that the phase diagram of the alloy computed using *ab initio* approximations are in agreement with experimental information. After reviewing the available phase equilibrium and thermodynamic data from different literatures for Ni-Al, two thermodynamic models were devised by Huang and Chang (1998) which have fewer and more reasonable model parameters as compared to others. They well explained the phase equilibrium and defect concentration of disordered fcc phase γ(-Ni, Al) are modeled by substitutional solution model and the ordered fcc γ' (-Ni_3Al) are modeled with two-sublattice model. Asta et al. (2001) studied the atomic and electronic structure and diffusion coefficients in liquid Ni-Al alloys by *ab initio* molecular dynamics simulations. Moreover, Adamiec (2007) determined the brittleness temperature range for the examined Ni_3Al alloy to be 1340 ^{0}C both for the liquidus heating stage and cooling stage. The thermodynamic database for the mixing properties of the considered system at different temperatures throughout the entire concentration range, however, is lacking in the literatures. Even though, Grigorovitch and Krylov (1998) used a new high- temperature calorimeter method to study the enthalpies of mixing of nickel-rich Al-Ni melts at 1823 K only in the concentration range Al< 0.22. They computed the other thermodynamic properties, such as integral enthalpy of mixing and activities of Al and Ni at very few temperatures on the basis of quasi-ideal solution model. Their results are in accordance with the findings of the present work. Recently, Yadav et al. (2016) have explained the thermodynamic and structural properties of Ni-Al liquid alloy at 1873 K using regular associated solution model and quasi-lattice model. Ahmed et al. (20018) presented self-consistent results of molecular dynamics simulations for the temperature and concentration dependence of the self-diffusion and interdiffusion coefficients, thermodynamic factor, Manning factor and the reduced heat of transport of the Ni-Al liquid alloy. But the phase determining mixing properties at different temperatures for the preferred system are unavailable in the literatures.

Eventually, we have extended STM by considering the linear temperature dependence of the interaction energy parameter to predict thermodynamic, structural and transport properties of the liquid alloy at

temperatures 1873 K, 1973 K, 2073 K and 2173 K, 1873 K being the melting temperature of the system. Redlich-Kister (R-K) polynomials [28, 29] have been associated with this approximation to determine the modeling parameters at different temperatures. The thermodynamic properties at different temperatures so computed have been correlated with RBM to predict the surface properties of the liquid alloy at above mentioned temperatures.

The brief procedures to obtain the theoretical modeling equations are presented in the Section 2, the results and discussion are outlined in the Section 3 and the conclusions of the work are highlighted in the Section 4.

2. Theoretical modeling equations

2.1 Thermodynamic properties

Simple statistical model is based upon pairwise interaction and conditional probabilities of occupation of neighbouring sites by the atoms of constituent elements which can be expressed in terms of interchange energy or interaction energy or ordering energy by applying grand partition function for binary alloys [30-32]. According to simple statistical method, the partition function for binary alloy of type A-B consisting of N_A and N_B atoms type of A and B element under the criteria $N_A+N_B = N$, where N=total number of each type atoms, is given by

$$\Xi=\sum_E q_A^{N_A}(T)\, q_B^{N_B}(T)\exp\left(\frac{\mu_A N_A+\mu_B N_B-E}{K_B T}\right) \quad (1)$$

where μ_i represents the chemical potential of i^{th} component and q_i^{Ni} represents atomic partition functions for i^{th} components provided i = A or B. K_B and T are Boltzmann constant and absolute temperature, E is the configurational energy of alloy. The thermodynamic relation between free energy of mixing (G_M) and excess free energy of mixing (G_M^{XS}) can be written as

$$G_M = G_M^{XS} + RT\sum_i x_i \log x_i \quad (2)$$

where x_i is the concentration of each component. The excess free energy of mixing is also given as [30-32]

$$\frac{G_M^{XS}}{RT} = \int_0^C \log\sigma^2 dx = x_A \log\gamma_A + x_B \log\gamma_B \quad (3)$$

where σ is expressed as

$$\sigma = (\beta + 2x_A - 1)\exp\left(\frac{-\omega}{zK_B T}\right)/2x_A \quad (4a)$$

$$\gamma_A = [(\beta - 1 + 2x_A)/x_A(1+\beta)]^{\frac{z}{2}} \quad (4b)$$

$$\gamma_B = [(\beta + 1 - 2x_A)/x_B(1+\beta)]^{\frac{z}{2}} \quad (4c)$$

$$\beta = 1 + 4x_A x_B[\exp(2\omega/ZK_B T) - 1]^{1/2} \quad (4d)$$

At equiatomic concentration ($x_A = x_B = 0.5$), the expression for G_M^{XS}/RT can be written as

$$\frac{G_M^{XS}}{RT} = \ln\{2^{Z/2}[1+\exp(-\omega/zK_B T)]^{-Z/2}\} \quad (5)$$

We have used "ω" notation for ordering energy of alloy and "Z" for co-ordination number. Then following Equation (2), the expression for free energy of mixing can be written as

$$G_M = NK_B T[x_A x_B \frac{\omega}{K_B T} + x_A \ln x_A + x_B \ln x_B] \quad (6)$$

The standard thermodynamic for heat of mixing (H_M) in terms of G_M can be expressed as

$$H_M = G_M - T\left(\frac{dG_M}{dT}\right) \quad (7)$$

Using Equation (5) in Equation (6), we get the expression for the heat of mixing as

$$H_M = NK_BT\left[x_Ax_B\frac{\omega}{K_BT} - \frac{1}{K_B}x_Ax_B\frac{d\omega}{dT}\right] \quad (8)$$

The activity (a_i) of the monomers of the binary liquid alloys in terms G_M of is given as [30]

$$NK_BT\ln a_i = G_M + (1-x_i)\left(\frac{\partial G_M}{\partial x_i}\right)_{T,P,N} \quad (9)$$

For each of the component (A and B) the expressions for activity are

$$\ln a_A = \ln x_A + x_B^2\frac{\omega}{K_BT} \quad (10)$$

$$\ln a_B = \ln x_B + x_A^2\frac{\omega}{K_BT} \quad (11)$$

2.2 Structural properties

The atomic arrangement of constituents of the liquid alloys can be investigated by using the parameters like concentration fluctuation in the long wave length limit ($S_{cc}(0)$) and Warren-Cowley short range order parameter (α_1) [17, 15, 33]. $S_{cc}(0)$ can be related with the two thermodynamic parameters namely, free energy of mixing (G_M) and activity (a_i) [15] as

$$S_{CC}(0) = K_BT\left(\frac{\partial^2 G_M}{\partial x^2}\right)^{-1}_{T,P,N} \quad (12a)$$

$$= x_Ba_A\left(\frac{\partial a_A}{\partial x_A}\right)^{-1} = x_Aa_A\left(\frac{\partial a_B}{\partial x_B}\right)^{-1} \quad (12b)$$

Using the Equation (5) in Equation (12a) yields

$$S_{CC}(0) = x_Ax_B\left[1+\frac{Z}{2\beta}(1-\beta)\right]^{-1} \quad (13)$$

where z represents the coordination number and we have taken it to be 10 for our work.

Moreover, the expression for the ideal value of $S_{CC}(0)$ can be given as [10, 15]

$$S_{CC}^{id} = x_Ax_B \quad (14)$$

Warren-Cowley short range order parameter (α_1) in terms of $S_{CC}(0)$ can be expressed as [10, 15]

$$\alpha_1 = \frac{(S-1)}{[S(Z-1)+1]} \quad (15)$$

where $S = S_{CC}(0)/x_Ax_B = S_{CC}(0)/S_{CC}^{id}(0)$ (16)

2.3 Surface properties

Following Kaptay (2015), according to Renovated Butler model, the surface tension (σ) of the binary liquid alloy of the type A-B can be given as [3, 14]

$$\sigma = \sigma_A^0\frac{\lambda_A^0}{\lambda_A} + \frac{RT}{\lambda_A}\ln\left(\frac{x_A^S}{x_A}\right) + \frac{\Delta G_{S,A}^{XS} - \Delta G_A^{XS}}{\lambda_A} = \sigma_B^0\frac{\lambda_B^0}{\lambda_B} + \frac{RT}{\lambda_B}\ln\left(\frac{x_B^S}{x_B}\right) + \frac{\Delta G_{S,B}^{XS} - \Delta G_B^{XS}}{\lambda_B} \quad (17a)$$

where σ_i^0 is the surface tension of the pure i^{th} component of the liquid mixture. λ_i^0 and λ_i are the molar surface areas of i^{th} component in the pure liquid and in the liquid solution respectively. $\Delta G_{S,i}^{XS}$ and ΔG_i^{XS} are the surface partial excess free energy and bulk partial free energy of i^{th} component; and x_i^S and x_i surface mole fraction and bulk mole fraction of the same component respectively in the liquid mixture such that $x_i^S + x_i = 1$. But the molar surface area of component in the pure liquid is equal to the molar surface area of the component in the liquid solution, i.e. $\lambda_i^0 = \lambda_i$ [3, 14].

The molar surface area of a pure liquid metal i is expressed as

$$\lambda_i = f\left(V_i^0\right)^{2/3}(N_{Av})^{1/3} \quad (17b)$$

where $N_{Av} = 6.022 \times 10^{23} mol^1$ is the Avogadro's number, V_i^0 is the molar volume of pure metal i at its melting temperature and f is the geometrical constant which is expressed as

$$f = \left(\frac{3\,f_b}{4}\right)^{2/3} \frac{\pi^{1/3}}{f_s} \quad (17c)$$

where f_b and f_s are the volume and surface packing fractions and their values depend upon the type of crystal structure of the pure components of the liquid alloys. The value of f is taken to be 1.06 for this work [3, 14, 34].

2.4 Transport properties

The transport properties of liquid alloys can be interpreted by using two parameters namely, viscosity (η) and ratio of mutual to intrinsic diffusion coefficients (D_M/D_{id}). According to simple statistical approach, viscosity (η) for liquid alloy can be expressed as [30, 31]

$$\eta = \eta_{id}\left[1 - x_A x_B\left(\frac{2\omega}{K_B T}\right)\right] \quad (18)$$

where η_{id} is ideal viscosity which is given by $\eta_{id} = (x_A\eta_A^0 + x_B\eta_B^0)$; η_i^0 stand for the viscosity of pure component in the liquid mixture.

The mutual diffusion coefficient (D_M) in terms of intrinsic diffusion coefficient (D_{id}) can be expressed as [35].

$$D_M = D_{id}\frac{d\ln a_i}{dx_i} \quad (19a)$$

where the terms carry their meanings as mentioned earlier. Above Equation can also be written as [10, 15, 29]

$$\frac{D_M}{D_{id}} = \left[\frac{S_{CC}^{id}(0)}{S_{CC}(0)}\right] \quad (19b)$$

where $D_M = x_A D_B + x_B D_A$; and D_A and D_B are self-diffusion coefficients of pure component.

Further, the expression for D_M/D_{id} can be expressed in term of ordering energy (ω) as

$$D_M = D_{id}\left[1 - x_A x_B\left(\frac{2\omega}{K_B T}\right)\right] \quad (20)$$

3 Results and Discussion

3.1 Thermodynamic properties

The thermodynamic model fit parameter, ω, called ordering energy for Ni-Al liquid alloy at 1875 K is computed using Equations (2-5) in order to explain the observed excess free energy of mixing (G_M^{XS}) [36]. The optimized value of ordering energy so obtained is $\omega = -7.03$ RT. The negative value of ω corresponds that the liquid system is found to be complete ordering in nature at least at its melting temperature, which is 1873 K. The compositional dependence of isotherm plots of the computed and observed G_M^{XS}/RT is portrayed in Figure 1. It can be observed that both of these values are in excellent agreement throughout the entire concentration range (Figure 1). The extremum values of G_M^{XS}/RT (=−2.0602, theoretical and = −2.0584, experimental [36]) at equiatomic concentration ($x_1 = x_2 = 0.5$) which corresponds that the system is strongly interacting and symmetric in nature at near to its melting temperature. The similar results were also obtained by Yadav et al. (2016) [1].

The ordering energy is assumed to be only temperature dependent in simple theory of mixing. The temperature dependent model parameter ($d\omega/dT$) is obtained from Equation (8) with the aid of above determined ω and experimental value of H_M [36] by successive approximation method. The best fit value

$d\omega/dT$ is found to be 47.25 for the system at 1873 K. Eventually, the theoretical value of H_M is computed from Equation (8) using the determined values of model parameters. Figure 1 displays the isotherm plots of experimental as well as theoretical values of H_M/RT as a function of concentration for the system. This figure further corresponds that both of these values are in good agreement. The minimum values of H_M/RT (=−3.1780, theoretical and −3.2111, experimental [36]) are found to be at $x_1 = x_2 = 0.5$. The theoretical findings thus communicates that the preferred system is symmetric with respect to H_M and there appears strong bonding between the constituent atoms of the complex at 1873 K.

Activity (a) is an important thermodynamic property which is directly measured from the experiments. The strength of compound formation tendency can also be interpreted on the basis of activity. Moreover, any observed deviation in the thermodynamic properties of the system can incorporated into the activity. The activities (a_{Ni} and a_{Al}) of both the monomers (Ni and Al) of the liquid system are computed using Equations (10 and 11) with the help of above determined model parameter. The isotherm plots of both the theoretical and experimental [36] values of a_{Ni} and a_{Al} as a function of concentration are presented in Figure 1. It can be observed that both the computed and observed values of a_{Ni} and a_{Al} are in excellent agreement at all concentrations of Ni ($x_{Ni} = 0.1 - 0.9$). The modeling equations and model fit parameter have not only explained G_M^{XS} and H_M but also have reproduced activity successfully. This establishes the validity of the simple theory of mixing.

To predict the mixing behaviours of the liquid system at different temperatures, above stated thermodynamic properties of the liquid system have been computed at 1873 K, 1973 K, 2073 K and 2173 K; 1873 K being its melting temperature. As the model parameter ω depends on temperature, their values at different temperatures have been computed assuming $d\omega/dT$ to be constant and using the following equations [3, 29]

$$d[\omega(T)]_{x_i} = \left(\frac{d\omega}{dT}\right) dT \quad (21a)$$

and, $$\omega(T_q) = \omega(T) + \left(\frac{d\omega}{dT}\right) dT \quad (21b)$$

where T_q (= 1973 K, 2073 K and 2173 K) are the temperatures of interests and T (=1873 K) is the melting temperature of the alloy. The ordering energies determined from Equation (21) at different temperatures are presented in Table 1. It can be observed that the negative values of ω gradually decreases with increase in temperature of the liquid alloy which indicates that the compound forming tendency gradually decreases at elevated temperatures.

Table 1: Ordering energies (ω) at different temperatures

Temperature (K)	ω ($Jmol^{-1}$)
1873	−109472
1973	−104747
2073	−100022
2173	−95296.9

The compositional dependence of activities of the free monomers Ni (a_{Ni}) and Al (a_{Al}) of the liquid alloy at different temperatures are then predicted using Equations (10 and 11) with the help of ω (determined from Equation (21)) and are plotted in Figure 2. It can be observed that the activities of the monomers of the liquid alloy increases with increase in its temperature indicating the decrease in the compound. forming tendency at elevated temperatures. The theoretical findings of this work are in accordance with that of others [3, 29, 37-39, 40].

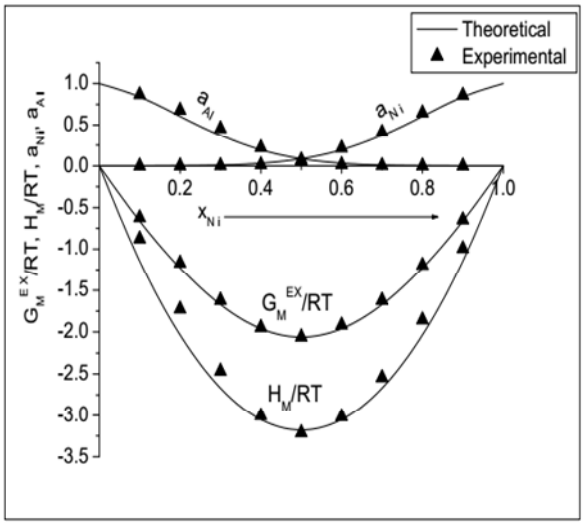

Fig. 1: Isotherm plots of excess free energy of mixing (G_M^{XS}), heat of mixing (H_M) and activities of Ni (a_{Ni}) and Al (a_{Al}) versus concentration of Ni (x_{Ni}) for Ni-Al liquid alloy at 1873 K.

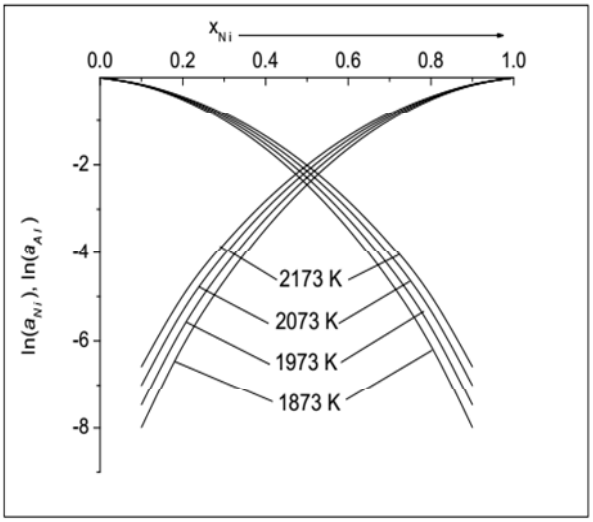

Fig. 2: The plots of activities of Ni ($\ln(a_{Ni})$) and Al ($\ln(a_{Al})$) versus concentration of Ni (x_{Ni}) at different temperatures for Ni-Al liquid alloy.

To predict the excess free energy of mixing at the above mentioned different temperatures, R-K polynomials are fitted. On the fundamentals of R-K polynomials, excess free energy of mixing (G_M^{XS}) as a function of concentration and temperature is expressed as [28, 29, 40, 41]

$$G_M^{XS}(x,T) = x_i \sum_{l=0}^{m} k_l(T)(x_1 - x_2)^l \quad (22)$$

where $k_l(T) = A_l + B_lT + C_lT\ln T + D_lT^2 + - - -$ and k_l has the same temperature dependence as G_M^{XS}. A, B, C and D are the fitting coefficients. The partial excess free energies of each monomers of the liquid system are expressed as

$$G_A^{XS}(x,T) = x_2^2 \sum_{l=o}^{m} k_l(T)[(1+2l)x_1 - x_2](x_1 - x_2)^{l-1} \quad (23a)$$

$$G_B^{XS}(x,T) = x_1^2 \sum_{l=o}^{m} k_l(T)[x_1 - x_2(1+2l)](x_1 - x_2)^{l-1} \quad (23b)$$

The optimized coefficients set of G_M^{XS} for Ni-Al liquid alloy are tabulated in the Table 2. These coefficients are obtained by the method of least square fitting.

Table 2: Optimized coefficient set of G_M^{XS} for Ni-Al liquid alloy

l	$A_l(10^6 \mathrm{Jmol^{-1}})$	$B_l(10^4 \mathrm{Jmol^{-1}K^{-1}})$	$C_l(10^3 \mathrm{Jmol^{-1}K^{-1}})$	$D_l(\mathrm{Jmol^{-1}K^{-2}})$
0	-80.3198	59.1000	-77.3906	18.6736
1	-1.92735	1.42178	-1.86200	0.449363
2	136.606	-100.755	131.948	-31.8373
3	59.3994	-43.8099	57.3728	-13.8431

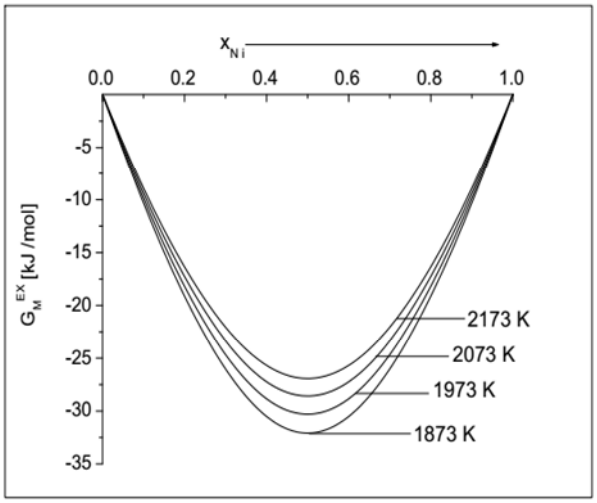

Fig. 3: The predicted values of G_M^{XS} versus concentration of Ni (x_{Ni}) for Ni-Al liquid alloy at different temperatures.

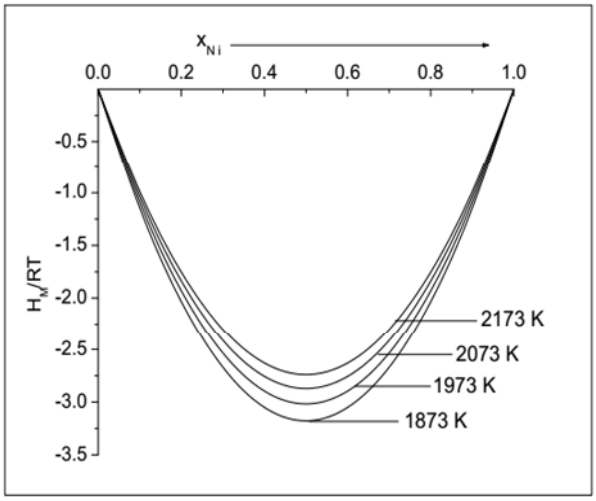

Fig. 4: The predicted values of H_M/RT versus concentration of Ni (x_{Ni}) for Ni-Al liquid alloy at different temperatures.

The excess free energy of mixing of the liquid alloy at above mentioned temperatures are then computed using Equation (22) with the help of the fitting coefficients in Table 1 and its compositional plots are displayed in Figure 3. It can be observed that the plots of G_M^{XS} gradually shallows up with the increase in the temperature of the system indicating the decrease in the values of G_M^{XS}. At $x_1 = x_2 = 0.5$, the computed values of G_M^{XS} are -32.0820, -30.2981, -28.5837 and -26.9302 kJmol^{-1} respectively at 1873 K, 1973 K, 2073 K and 2173 K. G_M^{XS} thus gradually decreases at higher temperature and is maximum at 1873 K which is the melting temperature of the system. The compound forming tendency, therefore, decreases at elevated temperatures and the system is found to be most interacting at its melting temperature. These results further strengthen the previous predictions of activity at different temperatures. The heat of mixing (H_M/RT) of the system at different temperatures are computed using Equations (7 and 8) with the aid of above determined values of G_M^{XS}. Figure 4 represents the compositional dependence of H_M/RT of the liquid alloy at different temperatures. Like G_M^{XS}, the plots of H_M/RT too gradually shallow up with the increase in the temperature of the system above 1873 K (Figure 4) which corresponds the decrease in H_M/RT. At $x_1 = x_2 = 0.5$, the computed values of H_M^{XS}/RT are -3.17830, -3.01721, -2.87166 and -2.73951 respectively at 1873 K, 1973 K, 2073 K and 2173 K. Theoretical predictions thus indicate that the strength of bonding between the atoms of the complex gradually decreases at elevated temperatures.

3.2 Structural properties

To have greater insight of the atomic arrangements in the disordered liquid mixture, we have computed concentration fluctuation in long wavelength limit $(S_{CC}(0))$ and Warren-Cowley short range order parameter ($Alpha_1 = \alpha_1$) in the frame work of STM at 1873 K. The ordering or compound forming

tendency and segregating or demixing tendency of the atoms of liquid mixture can also be interpreted on the basis of $S_{CC}(0)$ and α_1. At a given concentration and temperature, if $S_{CC}(0) < S_{CC}^{id}(0)$ for which $\alpha_1 < 0$, then the system shows ordering (hetero-coordinating) tendency and if $S_{CC}(0) > S_{CC}^{id}(0)$ for which $\alpha_1 > 0$, then it shows segregating (homo-coordinating) tendency.

Theoretical and ideal values of $S_{CC}(0)$ are computed using Equations (13 and 14) with the help of determined values of model parameters. The experimental values of $S_{CC}(0)$ are computed using Equation (12) and observed values of activity [36]. The theoretical values of α_1 are computed using Equations (15 and 16) with the help of determined values of essential ingredients. The isotherm plots of $S_{CC}(0)$ and α_1 as a function of concentration are portrayed in Figure 5. It can be observed that both the theoretical and experimental values of are less than ideal values, i.e. $S_{CC}(0) < S_{CC}^{id}(0)$ and $\alpha_1 < 0$ which correspond that the system is complete ordering in nature at its melting temperature. Moreover, both the theoretical and experimental values of $S_{CC}(0)$ are in good agreement which proves the validity of the theoretical modeling equations.

It has been already mentioned that we have also computed theoretical values of $S_{CC}(0)$ and α_1 at different temperatures within the constrained curtained of STM. These values are obtained using Equations (13-16) with the help of above determined parameters at different temperatures. The compositional and temperature dependence of $S_{CC}(0)$ and α_1 for the liquid alloy are presented in Figures 6 and 7. The values of $S_{CC}(0) < S_{CC}^{id}(0)$ and $\alpha_1 < 0$ at all concentrations and temperatures indicating that the ordering tendency still prevail in the liquid system. At $x_1 = x_2 = 0.5$, the deviation between $S_{CC}(0)$ and $S_{CC}^{id}(0)$ are found to be 0.209010, 0.204286, 0.199324 and 0.194113 at 1873 K, 1973 K, 2073 K and 2173 K respectively which predicts the decrease in the compound forming tendency of liquid alloys at elevated temperatures. However, this tendency is the maximum at 1873 K, the melting temperature of the alloy. Additionally, computed values of $S_{CC}(0)$ gradually gets closure to the ideal values at elevated temperatures. The perusal of Figure 7 communicates that the curves of α_1 gradually shallows up at elevated temperatures which indicates the decrease in compound forming tendency. Likewise, the values of α_1 at equiatomic composition are found to be -0.337710, -0.308860, -0.282290 and -0.257790 at 1873 K, 1973 K, 2073 K and 2173 K respectively predicting the similar nature as above.

3.3 Surface properties

The surface properties (surface tension (σ) and surface segregation (x_{Ni}^{S} and x_{Al}^{S}))give the information about various mechanical properties such as, the catalytic activity of alloy catalysts and wettability. The surface properties of the preferred liquid alloy at 1873 K have been studied in the frame work of Renovated Butler model (RBM) [8, 14, 19, 29, 34]. The theoretical values of σ, x_{Ni}^{S} and x_{Al}^{S} are computed using Equation (17). The surface partial excess free energy ($\Delta G_{S,i}^{XS}$) required herein is computed using the expression

$$\Delta G_{S,i}^{XS} = \beta(\Delta G_{i}^{XS}) \quad (24)$$

where the values of ΔG_{i}^{XS} are taken from Table 2 and the value of β is taken to be 0.8181 [8, 14, 19, 29, 34].

The molar surface areas of the monomers of the liquid alloy (λ_i) are computed using Equations (17b and 17c) by substituting $f = 1.06$ [3, 19]. The surface tensions of the pure components (σ_i^0) at the melting temperature (T=1873 K) of the liquid alloy are using the values from Table 3 and the following expression [42]

$$\sigma_i^0 = \sigma_0 + (T - T_0)\frac{d\sigma}{dT} \quad (25)$$

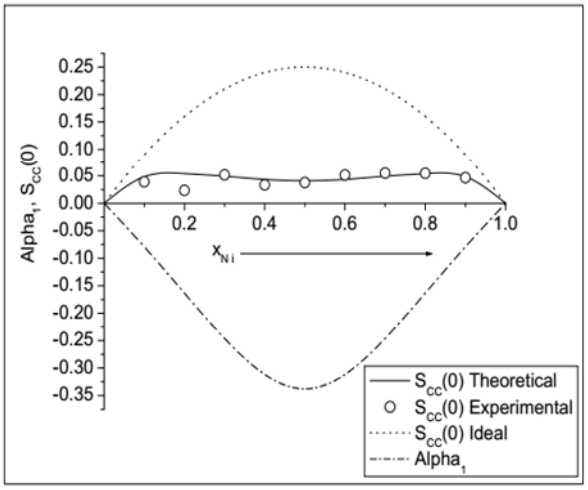

Fig. 5: The isotherm plots of computed values of $S_{CC}(0)$ and α_1 versus concentration of Ni (x_{Ni}) for Ni-Al liquid alloy at 1873 K.

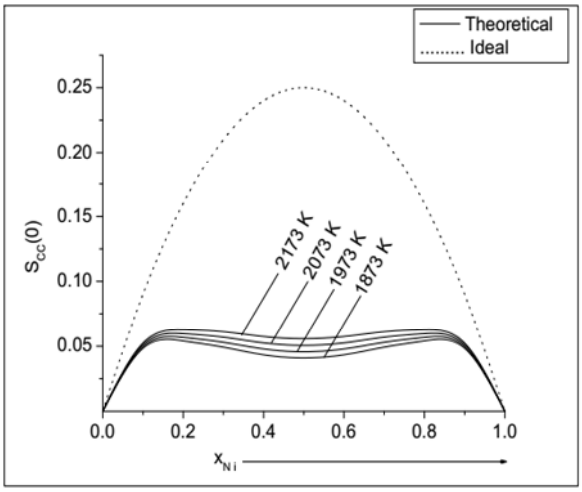

Fig. 6: The computed values of $S_{CC}(0)$ versus concentration of Ni (x_{Ni}) for Ni-Al liquid alloy at different temperatures.

where σ_0 is the surface tension of the pure component at its melting temperature, T_0 is its melting temperature in absolute scale and $d\sigma/dT$ is the temperature derivative of the surface tension. The molar volumes of the pure components (V_i^0) are determined from the ratio of their atomic masses to respective densities (m/ρ). The density of each component of the liquid mixture at T=1873 K is computed using the parameters from Table 3 and the expression [42]

$$\rho = \rho_0 + (T - T_0)\frac{d\rho}{dT} \quad (26)$$

where ρ_0 is the density of the pure component at its melting temperature (T_0) and $d\rho/dT$ is the temperature derivative of the density.

Table 3: Input parameters for surface tension (σ) and viscosity (η) [42]

Metal	T_0 (K)	Density		Surface tension		Viscosity	
		ρ_0 (kg m^{-3})	$d\rho/dT$ (kg m^{-3}K^{-1})	σ_0 (mNm^{-1})	$d\sigma/dT$ (mNm^{-1}K^{-1})	η_0 (mNsm^{-2})	E (kJmol^{-1})
Ni	1727	7905	−1.160	1778	−0.38	0.1663	50.2
Al	933	2385	−0.280	914	−0.35	0.1492	16.5

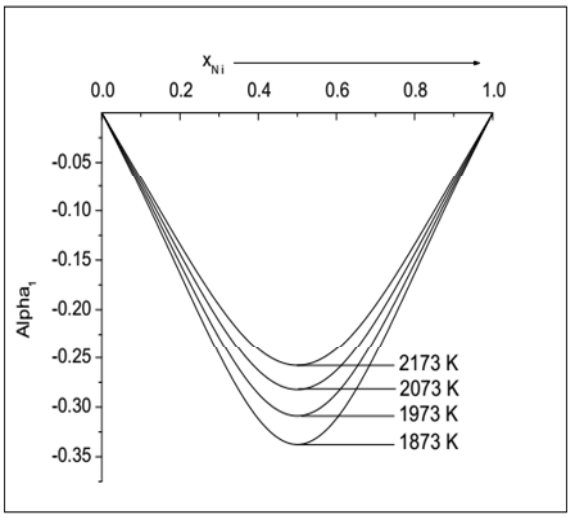

Fig. 7: The computed values of α_1 versus concentration of Ni (x_{Ni}) for Ni-Al liquid alloy at different temperatures

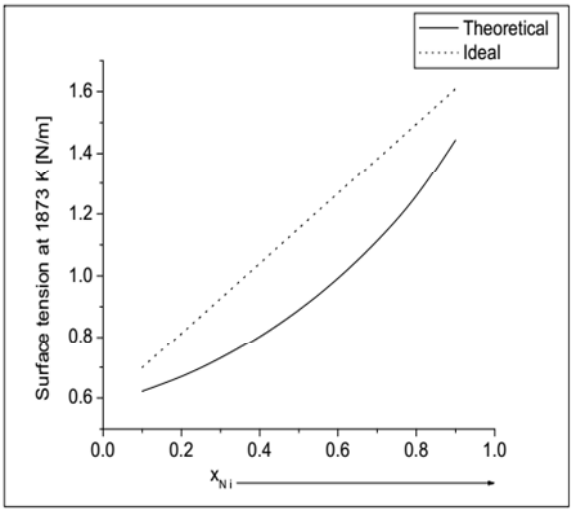

Fig. 8: The computed values of σ versus concentration of Ni (x_{Ni}) for Ni-Al liquid alloy at 1873 K.

The isotherm graphical representations of surface tension (σ) and surface concentrations (x_{Ni}^S and x_{Al}^S) as a function of concentration for the system at 1873 K are portrayed in Figures 8 and 9 respectively. The surface tension of the system is found to be less than ideal value throughout the entire concentrations (Figure 8). The perusal of Figure 9 corresponds that the surface concentration of Al is greater than its ideal value and that of Ni is less than that of its ideal value indicating that Al atoms segregate on the surface region whereas Ni atoms remain in the bulk phase of the liquid mixture at 1873 K.

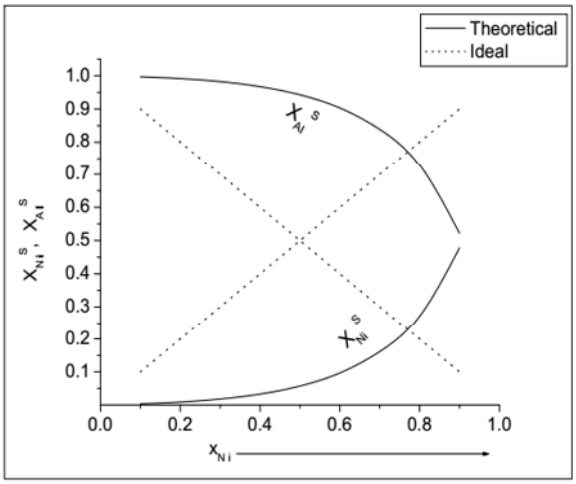

Fig. 9: The compositional dependence of isotherm plots of x_{Ni}^S and x_{Al}^S for Ni-Al liquid alloy at 1873 K.

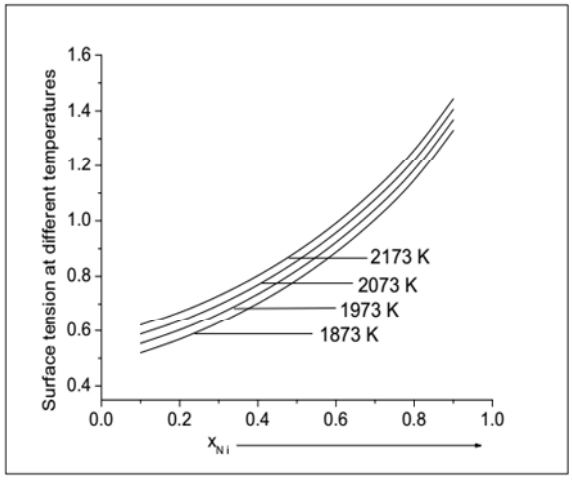

Fig. 10: The compositional dependence of computed values of σ for Ni-Al liquid alloy at different temperatures.

The theoretical values of σ, x_{Ni}^{S} and x_{Al}^{S} for the preferred liquid alloys at above mentioned different temperatures are computed using Equations (17, 24-26) with the help of ingredients from Tables 2 and 3. The compositional and temperature dependence of σ, x_{Ni}^{S} and x_{Al}^{S} are plotted in Figures 10, 11 and 12 respectively. Figure 10 predicts that σ of the system gradually decreases with increase in its temperature which further strengthen the earlier findings of thermodynamic and structural properties. It can be observed that the predicted values of x_{Ni}^{S} gradually increases (Figure 11) whereas that of x_{Al}^{S} gradually decreases with increase in the temperature of the system. More precisely, Ni atoms gradually move from the bulk phase to the surface whereas Al atoms gradually move from surface phase to the bulk in order to maintain equilibrium. Moreover, the predicted values of x_{Ni}^{S} and x_{Al}^{S} gradually approaches their ideal values at elevated temperatures; and are accordance with findings of others [3, 29, 37-39, 40].

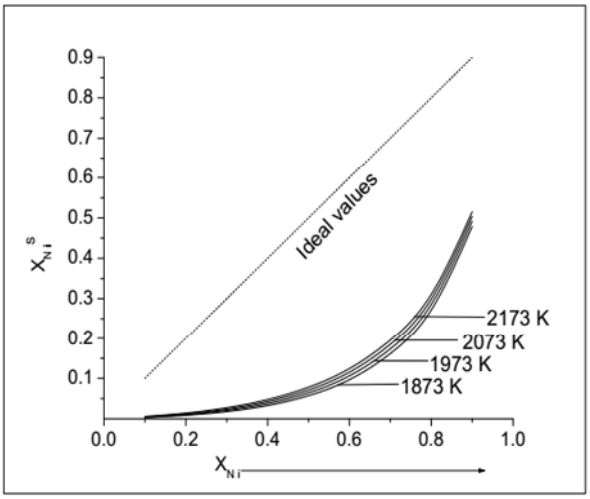

Fig. 11: The compositional dependence of computed values of x_{Ni}^{S} for Ni-Al liquid alloy at different temperatures.

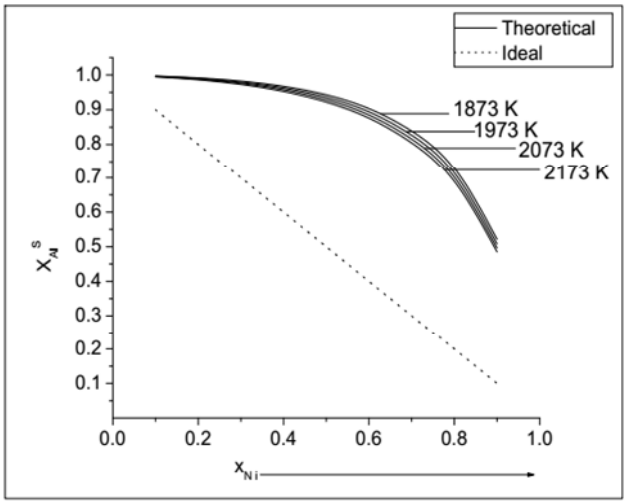

Fig. 12: The compositional dependence of computed values of x_{Al}^{S} for Ni-Al liquid alloy at different temperatures

3.4Transport properties

In transport properties, we have computed viscosity (η) and ratio of mutual to intrinsic diffusion coefficients (D_M/D_{id}) for the preferred system at 1873 K and also at above mentioned different temperatures on the floor of STM. Theoretical values of η for the system at 1873 K and different temperatures are computed using Equations (18) with the help of essential parameters from Tables 1 and 3. The plots of η as a function of concentration and temperature are portrayed in Figures 13 and 14.

The perusal of Figure 13 indicates that the viscosity of the liquid alloy at its melting temperature (1873 K) is less than its ideal value at all concentrations. It increases rapidly with increase in the concentration of Ni till about $x_{Ni} = 0.75$ and then decreases. The viscosity of the system decreases gradually with increase

in its temperature as one expects. As viscosity depends upon H_M of the liquid alloy, similar trends are followed by their plots at elevated temperatures.

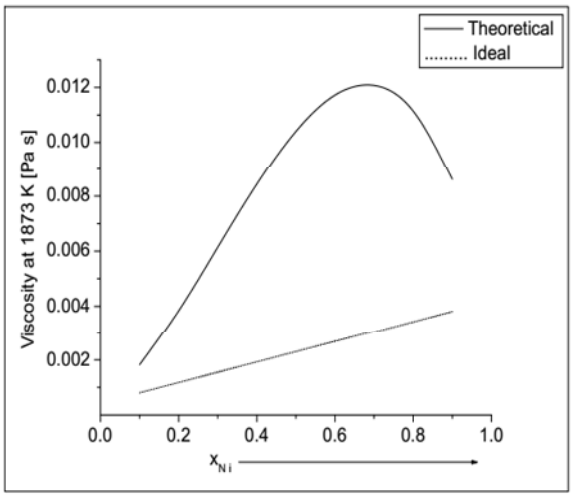

Fig. 13: The compositional dependence of isotherm plot of viscosity (η) for Ni-Al liquid alloy at 1873 K.

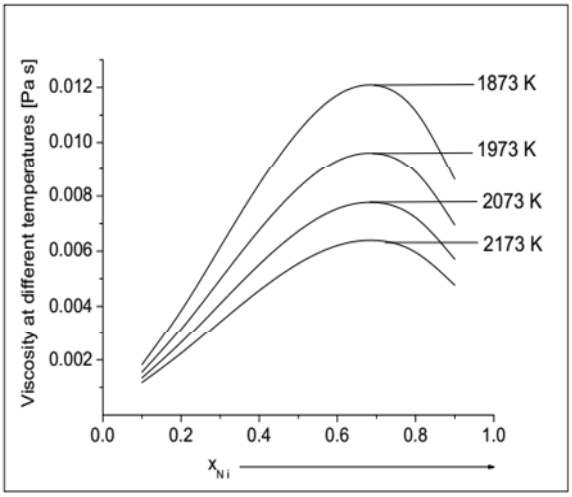

Fig. 14: The compositional dependence of predicted values of η for Ni-Al liquid alloy at different temperatures.

Theoretical values of D_M/D_{id} at 1873 K and also at higher temperatures are obtained using Equation (20) and the values of parameters from Table 1. The graphical representations of values so computed are displayed in Figures 15 and 16.

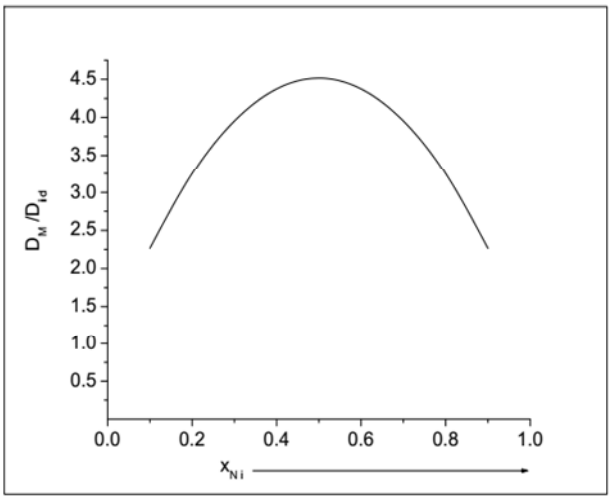

Fig. 15: The computed values of D_M/D_{id} versus concentration of Ni (x_{Ni}) for Ni-Al liquid alloy at 1873 K.

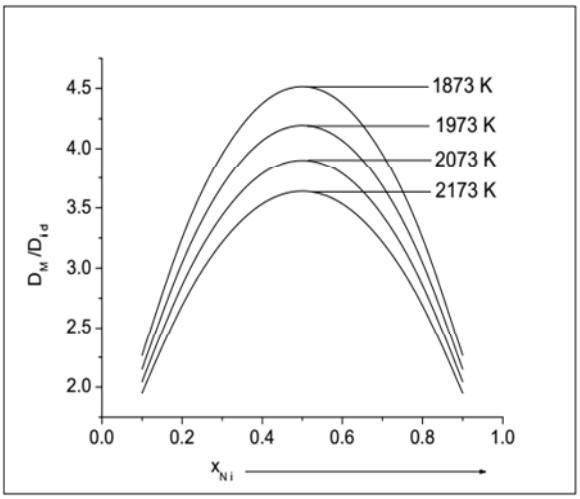

Fig. 16: The computed values of D_M/D_{id} versus concentration of Ni (x_{Ni}) for Ni-Al liquid alloy at different temperatures.

The study of D_M/D_{id} helps to understand the compound forming or ordering tendency of the liquid alloy. At given temperature and concentration, if $\frac{D_M}{D_{id}} > 1$, then the liquid alloy shows ordering nature and if $\frac{D_M}{D_{id}} < 1$, then it shows segregating nature. The perusal of Figure 15 notifies that $\frac{D_M}{D_{id}} > 1$ throughout the entire concentrations at the melting temperature of the system indicating that there is strong tendency towards compound formation at this temperature. However, it can be observed that the predicted values of D_M/D_{id} gradually decreases with increase in the temperature of the system which corresponds that the compound forming tendency gradually declines at elevated temperatures.

4. Conclusions

The mixing behaviours of the preferred liquid alloy have been successfully explained and predicted at its melting and higher temperatures on the basis of theoretical modeling equations. Theoretical investigations forecast that the system shows strong tendency towards compound formation at least at its melting temperature, however, this tendency gradually declines at higher temperatures. More precisely, the system shows ideal behaviours with regards to mixing properties at elevated temperatures.

Acknowledgements

We are grateful to UGC, Nepal for providing financial support through Faculty Research Grants to pursue this work.

References

[1] S. K. Yadav, S. Lamichhane, L.N. Jha, N.P. Adhikari, D. Adhikari, Mixing behaviour of Ni-Al melt at 1873 K, Phys. Chem. Liq. 54 (2016) 370. doi.org/10.1080/00319104.2015.1095640.

[2] M. P. Tresa, T. Sammy, Nickel-based super alloys for advanced turbine engines: chemistry, microstructure and properties, J. Propul Powe 22 (2006) 361. doi.org/10.2514/1.18239.

[3] S.K. Yadav, L.N. Jha, I.S. Jha, B.P. Singh, R.P. Koirala, D. Adhikari, Prediction of thermodynamic and surface properties of Pb-Hg liquid alloys at different temperatures, Phil. Mag. 96 (2016) 1909. doi.org/10.1080/14786435.2016.1181281.

[4] K. Hoshino, W.H. Young, On the electrical resistivity of the liquid Li-Pb alloy, J. Phys. F: Metal Phys. 10 (1980) 1365. doi.org/10.1088/0305-4608/10/7/003.

[5] H. Ruppersberg, H.J. Reiter, A simple local pseudopotential for lithium, J. Phys. F: Metal Phys. 12 (1982) 1311. doi.org/10.10888/0305-4608/12/7/005.

[6] A. B. Bhatia, W.H. Hargrove, Concentration fluctuations and thermodynamic properties of some compound forming binary molten systems, Phys. Rev. B 10 (1974) 3186. doi.org/10.1103/PhysRevB.10.3186.

[7] A.S. Jordan, A theory of regular associated solution applied to the liquidus curve of the Zn−Te and Cd−Te system, Metall. Trans. 1 (1970) 239.

[8] D. Adhikari, I.S. Jha, B.P. Singh, Structural asymmetry in liquid Fe–Si alloys, Phil. Mag. 90 (2010) 2687. doi.org/10.1080/14786431003745302.

[9] S. Lele, P. Ramchandrarao, Estimation of complex concentration in a regular associated solution Metall. Met. Trans. 12 (1981) 659. doi.org/10.1007/BF02654134.

[10] S.K. Yadav, L.N. Jha, D. Adhikari, Thermodynamic and structural properties of Bi-based liquid alloys, Physica B: Cond. Mat. 475 (2015) 40. doi.org/10.1016/j.physb.2015.06.015.

[11] S.K. Yadav, L.N. Jha, D. Adhikari, Thermodynamic, structural, transport and surface properties of Pb-Tl liquid alloy, Bibechana 13 (2016) 100. doi.org/10.3126/bibechana.v13i0.13443.

[12] P. J. Flory, Thermodynamics of High Polymer Solutions, J. Chem. Phys. 10 (1942) 51. doi.org/10.10631/1.1723621.

[13] R. Novakovic, Thermodynamics, surface properties and microscopic functions of liquid Al–Nb and Nb–Ti alloys, J. Non-Cryst. Solids, 356 (2010) 1593. doi.org/10.1016/j.jnoncrysol.2010.05.055.

[14] G. Kaptay, Partial Surface Tension of Components of a Solution, Langmuir 31 (2015) 5796. doi.org/10.1021/acs.langmuir.5b00217.

[15] S.K. Yadav, L.N. Jha, D. Adhikari, Thermodynamic and structural behaviour of Mg-Ga melt at 923 K, J. Adv. Phys. 3 (2014) 248. doi.org/ 10.1166/jap.2014.1133.

[16] A.B. Bhatia, R.N. Singh, A quasi-lattice theory for compound forming molten alloys, Phys. Chem. Liq. 13 (1984) 177. doi.org/10.1080/00319108408080778.

[17] A.B. Bhatia, W.H. Hargrove, Concentration fluctuations and thermodynamic properties of some compound forming binary molten systems Phys. Rev., 10 (1974) 3186. doi.org/10.1103/PhysRevB.10.3186.

[18] S.K. Yadav, L.N. Jha, D. Adhikari, Thermodynamic and structural behaviour of Tl-Na liquid alloy, Bibechana, 12 (2015) 20. doi.org/ 10.3126/bibechana.v12i0.11784.

[19] G. Kaptay, Modelling equilibrium grain boundary segregation, grain boundary energy and grain boundary segregation transition by the extended Butler equation, J. Mater. Sci. 51 (2016) 1738. doi.org/10.1007/s10853-015-9533-8.

[20] I. Ansara, B. Sundman, P. Willemin, Thermodynamic modeling of ordered phases in the N-Al system, Acta Metall. 36 (1988) 977. doi.org/10.1016/0001-6160(88)90152-6.

[21] M. Maret, T. Pomme, A. Pasturel, P. Chieux, Structure of liquid $Al_{80}Ni_{20}$ alloy, Phys. Rev. B 42 (1990) 1598. doi.org/10.1103/PhysRevB.42.1598.

[22] A. Pasturel, C. Colinet, A.T. Paxtonl, M. van Schilfgaarde, First-principles determination of the Ni-Al phase diagram, J. Phys.: Condens. Matter 4 (1992) 945. doi.org/10.1088/0953-8984/4/005.

[23] W. Huang, Y.A. Chang, A thermodynamic analysis of the Ni-Al system, Intermetallics 6 (1998) 487. doi.org/10.1016/S0966-9795(97)00099-X.

[24] K.V. Grigorovitch, A.S. Krylov, Thermodynamics of liquid Al-Ni alloys, Thermochimica Acta 314 (1998) 255. doi.org/10.1016/S0040-6031(98)00262-7.

[25] M. Asta, V. Ozolins, J.J. Hoyt, M. van Schilfgaarde, Ab initio molecular-dynamics study of highly nonideal structural and thermodynamic properties of liquid Ni-Al alloys, Phys. Rev. B 64 (2001) 020201-1. doi.org/10.1103/PhysRevB.64.020201.

[26] J. Adamiec, Ni_3Al alloy's properties related to high temperature brittleness, Arch. Mat. Sci. Eng. 28 (2007) 333.

[27] T. Ahmed, W.Y. Wang, R. Kozubski, Z.K. Liu, I.V. Belova, G.E. Murch, Interdiffusion and thermotransport in Ni-Al liquid alloys, Phil. Mag. (2018). doi.org/ 10.1080/14786435.2018.1479077.

[28] O. Redlich, A. Kister, Thermodynamics of Nonelectrolyte Solutions - x-y-t relations in a Binary System, Indust. Eng. Chem. 40 (1948) 345. doi.org/10.1021/ie50458a035.

[29] S.K. Yadav, L.N. Jha, D. Adhikari, Modeling equations to predict the mixing behaviour of Al-Fe liquid alloy at different temperatures, Bibechana, 15 (2018) 60. doi.org/10.3126/bibechana.v15i0.18624.

[30] I. Koirala, I.S. Jha, B.P. Singh, D. Adhikari, Thermodynamic, transport and surface properties in In-Pb liquid alloys, Physica B: Cond. Mat. 423 (2013) 49. doi.org/10.1016/j.physb.2013.04.051.

[31] R.N. Singh, I.K. Mishra, V.N. Singh, Local order in Cd-based liquid alloys, J. Phys. Cond. Mat. 2 (1990) 8457. doi.org/10.1088/0953-8984/2/42/022.

[32] I. Koirala, B.P. Singh, I.S. Jha, Theoretical assessment on segregation nature of liquid In-Tl alloys, J. Non-cryst. Solids 398 (2014) 26. doi.org/10.1016/j.noncrysol.2914.04.018.

[33] J.M. Cowley, An Approximate Theory of Order in Alloys, Phys. Rev. 77 (1950) 669. doi.org/10.1103/PhysRev.77.669.

[34] G. Kaptay. Modelling equilibrium grain boundary segregation, grain boundary energy

and grain boundary segregation transition by the extended Butler equation, J. Mat. Sci. 51 (2016) 1738. doi.org/10.1007/s10853-015-9533-8.

[35] L.S. Darken, R. Gurry, Physical Chemistry of Metals, McGraw Hill, New York, (1953).

[36] P.D. Desai, Thermodynamic properties of selected binary aluminum alloy systems, J. Phys. Chem. Ref. Data 16 (1987) 109. doi.org/10.1063/1.555788.

[37] F. Aqra, Ah. Ayyad, F. Takrori, Model calculation of the surface tension of liquid Ga−Bi alloy, App. Surf. Sci. 257 (2011) 3577. doi.org/10.1016/j.apsusc.2010.11.079.

[38] O.E. Awe, Y.A. Odusote, L.A. Hussain, O. Akinlade, Temperature dependence of thermodynamic properties of Si−Ti binary liquid alloys, Thermochimica Acta 519 (2011) 1. doi.org/10.1016/j.tca.2011.02.028.

[39] S.K. Yadav, L.N. Jha, D. Adhikari, Theoretical modeling to predict the thermodynamic, structural, surface and transport properties of the liquid Tl-Na alloys at different temperatures, JNPS 4 (2017) 101.

[40] R.N. Singh, F. Sommer, Segregation and immiscibility in liquid binary alloys, Rep. Prog. Phys. 60 (1997) 57. doi.org/101088/0034-4885/60/1/003**.**

[41] S.K. Yadav, L.N. Jha, A. Dhungana, U. Mehta, D. Adhikari, Thermo-physical properties of Al-Mg alloy in liquid state at different temperatures, Mater. Sci. Appl. 9 (2018) 812. doi.org/10.4236/msa.2018.910058**.**

[41] E.A. Brandes, G.B. Brook, Smithells Metals Reference Brook, Jordanhill, Oxford:Butterwarth-Heinemann (1992).